

The Eurasia Proceedings of Science, Technology, Engineering & Mathematics (EPSTEM), 2024

Volume 32, Pages 575-590

IConTES 2024: International Conference on Technology, Engineering and Science

The Effect of High Temperatures on the Compression and Flexural Characteristics of Recycled Fiber-Reinforced Concrete

Atlaoui Djamal

University 'Mouloud Mammeri' of Tizi Ouzou

Bouafia Youcef

University of 'Mouloud Mammeri' of Tizi Ouzou

Ghouilem Kamel

University of Mouloud Mammeri, Tizi Ouzou

Abstract: The objective of this experimental study is to examine the behavior of concrete reinforced with metallic fibers (CMF) and polypropylene fibers (CPPF) subjected to high temperatures, as well as the effect of temperature variations on their mechanical properties, by evaluating the residual mass loss as well as the residual compressive and flexural strength. Two optimal fiber contents were selected for this study: $W = 0.2\%$ in compression and $W = 0.8\%$ in flexure, while a control concrete ($W=0\%$) of the same composition serves as a reference. The fibers are characterized by their mechanical strength and pull-out resistance. The concrete composition is determined using the experimental method known as the "Dreux-Gorisse" method. Compression tests are carried out on cylinders with a diameter of $\varnothing 16$ cm and a height of H32 cm, while flexural tests are performed on prismatic specimens with dimensions $[10 \times 10 \times 40]$ cm³. Fiber-reinforced concretes are subjected to different heating-cooling cycles, reaching maximum temperatures of 600°C and 800°C at 28 days of age. This study revealed that the residual compressive and flexural strength of fiber-reinforced concretes exposed to very high temperatures of 600°C and 800°C decreases compared to concretes not exposed to such temperatures (20°C). For all temperatures studied, concrete reinforced with metallic fibers (CMF) showed significantly higher strength than concrete reinforced with polypropylene fibers (CPPF). At 800°C, both metallic fiber concretes and polypropylene fiber concretes exhibited networks of microcracks, but no spalling occurred.

Keywords: Concrete, Flexion, Metal fibers, High temperature, Compression

Introduction

Recent incidents involving fires in concrete structures highlight the detrimental effects of high temperatures on the material's integrity. Various examples, whether it be tunnels or buildings, demonstrate significant damages, such as concrete spalling or structural collapses, caused by fires. Ensuring the safety of people, structures, and the environment in the face of such fire events requires particular attention during the design of constructions. Due to the complex composition of concrete, understanding the phenomena that occur during fires is essential for accurately assessing the fire resistance of structures (post-fire). Experimental studies have been conducted to replace the reinforcement in reinforced concrete with fibers capable of providing the concrete with good resistance to tension, bending, compression, and shear (Atlaoui & Gouilem, 2023; Atlaoui & Bouafia, 2017; Djebali et al., 2011; Atlaoui & Bouafia, 2008; Bouafia et al., 2012; Djebali et al., 2011; Tadepalli et al., 2013; Sorensen et al., 2014; Wang & Wang, 2013; Serbescu et al., 2015; Djebali et al., 2011; Atlaoui et al., 2023). Numerous research studies have focused on managing high temperatures to assess the residual performance of concrete under such conditions. The results suggest that incorporating fibers into the cement mix can improve various properties of concrete, such as tensile and flexural strength, as well as other physical characteristics.

- This is an Open Access article distributed under the terms of the Creative Commons Attribution-Noncommercial 4.0 Unported License, permitting all non-commercial use, distribution, and reproduction in any medium, provided the original work is properly cited.

- Selection and peer-review under responsibility of the Organizing Committee of the Conference

© 2024 Published by ISRES Publishing: www.isres.org

According to the literature, the addition of polypropylene fibers is particularly effective in enhancing the behavior of concrete exposed to high temperatures (Hager, 2004; Noumowe, 2005; Pliya, 2010). Researchers have also noted that the use of steel or polypropylene fibers can enhance the resistance of reinforced concrete structures to high temperatures, with a preference for polypropylene fibers due to their ability to improve concrete strength and behavior in case of fire. Although the addition of steel fibers also offers advantages over traditional concrete, it is noted that polypropylene fibers generally outperform the achieved performances. The incorporation of these fibers has been recommended by several studies (Hager, 2004; Serrano et al., 2016; Yermak et al., 2017) to enhance both the initial and residual strength of concrete, while reducing the risk of spalling at high temperatures. Numerous research studies have been conducted on the behavior of fiber-reinforced concrete when exposed to fire. (Mohamed, 2007). In one study, the mechanical characteristics of fiber-reinforced concrete samples were examined after subjecting them to high temperatures up to 800°C. (Tai et al., 2011) The results revealed that after heating, the residual compressive strength of fiber-reinforced concrete increased between 200 and 300°C, then experienced a significant decrease when the samples were exposed to temperatures higher than 300°C up to 800°C.

The impact of high temperatures (Sana & Abdul, 2013) on the mechanical characteristics of fiber-reinforced concrete, according to another study, was primarily observed in terms of compressive strength, flexural strength, and cracking tensile strength. Overall, the results demonstrated that beyond 400°C, the decrease in these strengths became more pronounced. At 600°C, the compressive strength, flexural strength, and cracking tensile strength were affected.

The heating rate plays a crucial role in the thermal stability of concrete. The higher the heating rate, the greater the risk of spalling. Characterization tests conducted by Coke and Venstermans (1977) on concrete samples subjected to heating-cooling cycles at a rate of 1°C/min resulted in spalling of the samples, while those heated at a rate of 0.1°C/min did not spall. A slower temperature rise rate limits the formation of saturated zones and reduces temperature gradients. Rapid heating of the concrete surface creates high thermal gradients, thus inducing thermal stresses. These stresses, whether in compression or tension, can lead to concrete spalling.

Characterizing concrete involves considering compressive strength, which generally decreases with increasing temperatures. A recent study reference Hager (2004) conducted hot compression tests on various concrete samples, including different formulations with water-to-cement (W/C) ratios of 0.3, 0.4, and 0.5. Data analysis revealed three distinct phases in the evolution of strength as a function of temperature. The first phase, ranging from ambient temperature to 100°C, showed a relative reduction in compressive strength of 20% to 30%. The second phase, between 100°C and 250°C, exhibited an increase in strength compared to 100°C, although this increase was observed only for high-performance concretes up to 400°C. This delayed increase, supported by other studies references (Castillo & Durrani, 1990; Pimienta, 2000 ; Tshimanga, 1992), can be attributed to the low permeability of high-performance concretes, which delays water release. Finally, the last phase, beyond 400°C for high-performance concretes and 250°C for other concretes, showed a continuous decrease in strength, accompanied by the appearance of initial cracks due to differential deformation between the aggregates and the paste.

Residual compression tests have also reported a similar trend for concrete. Other researchers (references (Diederichs & Jumpanen, 1992; Phan, 2002) have examined the evolution of compressive strength as a function of temperature and divided it into two ranges. The first range, from ambient temperature to 250-400°C, showed a slight decrease, stability, or even an increase in strength. In the second range, from the intermediate limit up to 600°C, a constant decrease in compressive strength was observed. Both hot and post-cooling tests revealed a decrease in compressive strength between 100°C and 200°C.

Since compression failure is due to surpassing shear stresses, the decrease in bonds between hydrates can create micro defects favoring sliding. An increase in compressive strength has been observed between temperatures of 250°C and 350°C (or even 400°C). This phenomenon could result from the loss of water from the material, possibly followed by a re-increase in bonding forces between hydrates and an increase in surface energies (Dias et al., 1990). These mechanisms overall contribute to an increase in compressive strength. Beyond 350°C (or 400°C), the strength gradually decreases. From this temperature threshold, the behavior of concrete is influenced by the hydroxylation of portlandite and by the differential thermal expansion between the cement paste (shrinkage) and the aggregates (expansion).

Our research aims to address these questions by focusing on the study of the compression and flexural behavior of steel fiber-reinforced concrete (CMF) and polypropylene fiber-reinforced concrete (CPPF). The objective of this experimental study is to analyze and gain a better understanding of the behavior of fiber-reinforced

concretes at high temperatures (600°C and 800°C) and the impact of temperature evolution on their mechanical properties. We assess these changes by measuring the residual mass loss as well as residual compressive and flexural strength. In the scope of this study, we use two optimal fiber contents for compression tests (W=0.2%) and flexural tests (W=0.8%), as well as a control concrete BT (W=0%) serving as a reference without fibers (W=0%). The steel fiber-reinforced concrete, polypropylene fiber-reinforced concrete, and fiber-free concrete (W=0%) undergo various heating-cooling cycles up to maximum temperatures of 600°C and 800°C at the age of 28 days.

Materials and Methods

Materials

Characteristics of the Fibers Used in the Study

The metallic fibers (MF) and polypropylene fibers (PPF) used in the study are locally sourced fibers derived from recycling. The metallic fibers are in the form of metal chips (waste from machining steel parts) collected from the National Company of Industrial Vehicles (SNVI) in Algeria. They have a somewhat wavy geometric shape, which promotes their anchoring in concrete. Three fiber lengths were used (4, 5, and 6 cm) with 3, 5, and 6 undulations (spirals). Three tests for each type of combination were conducted. The anchoring of the ends of the metallic fibers in the grips of the hydraulic press is enhanced by a glass fiber resin. The appearance of the fibers used, the anchoring of the ends of the metallic fibers, and the mechanical and geometric properties of the fibers used are illustrated respectively in Figure 1, Figure 2, and Table 1.

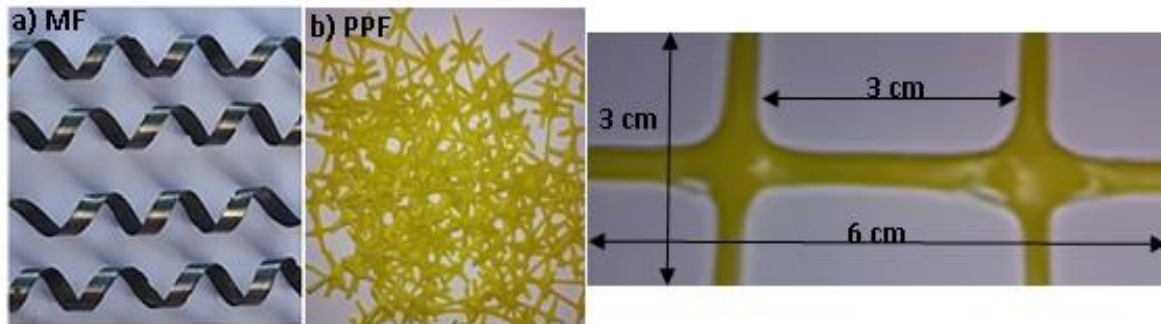


Figure 1. View of the fibers: a) metallic fibers; b) polypropylene fibers; c) dimensions of polypropylene fibers



Figure 2. Anchorage system

Table 1. Characteristics of mechanical properties of fibers under the study

Types of fibers	L (cm)	l (cm)	e_p (cm)	Φ (cm)	σ_e (MPa)	γ (g /cm ³)
Metal fibers	6	0.02	0.06	0.8275	7.87	
Polypropylene fibers	6	0.3	0.3	/	16.92	0.95

Mass of different fiber contents for 1m³ concrete are given by Table 2.

Table 2. Mass different contents of fibers for concrete 1m³

Fiber volume fractions W (%)	Metal fibers	Polypropylene fibers
Weights for 1m ³ of concrete) (kg)	7 870	950

Procedure for the Preparation of Test Specimens and Mixing Procedure

The concrete used in this study includes CPJ-CEMII/B 42.5 R NA 442 type cement, class 42.5, sourced from the Lafarge region in Msila, Algeria, in accordance with standard NF EN 196-6 (AFNOR, 2018). The aggregates used are from the Tizi Ouzou region, specifically quarry rocks. These aggregates are crushed, and the particle size classes used are 0/3 mm, 3/8 mm, and 8/15 mm, all washed and oven-dried. Particle size analysis by sieving was conducted according to standard NF P18-560, using a sieve with an adjustable frequency of 50 Hz. The concrete composition per cubic meter was formulated using the Dreux-Gorisse method (Dreux & Festa, 2007). Figure 3 presents the particle size distribution curves for each type of aggregate. The mixing process was carried out using a vertical-axis mixer with a capacity of 65 L. Table 3 provides a summary of the mixing proportions for 1 m³ of concrete for all batches used in this test program. The concrete mixing was done in a rotary mixer, strictly following the following mixing procedure:

- Introduction of sand, aggregates, and cement, mixed for 60 seconds.
- Introduction of water, mixed for 40 seconds.
- Introduction of the water reducer, mixed for 30 seconds.
- For concrete mixes with fibers, they are introduced last, in small quantities, with a 20-second mix after each addition.

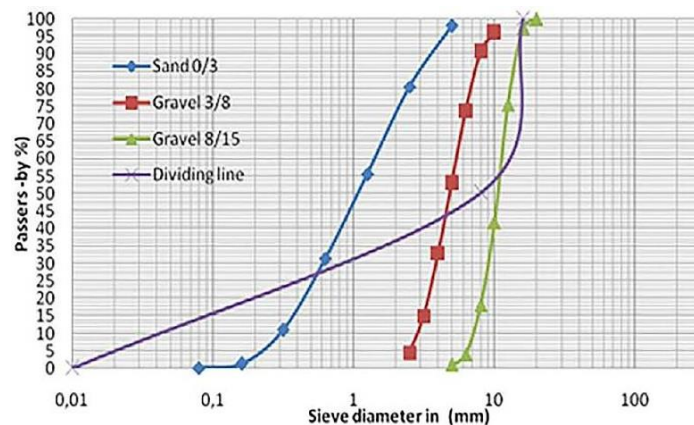


Figure 3. Particle size curve

Table 3. Proportions of the concrete mix used for 1m³

Ingredient	Amount (kg/m ³)
coarse aggregate (8/15) (kg)	895.00
Medium aggregate (3/8) (kg)	171.00
Sand (0/3) (kg)	753.00
Water (W) (kg)	207.00
Cement CPJ CEMII/A 42.5 (C) (kg)	380.00
Superplasticizer (0.5% of cement weight) (ml)	190.00

Methods

Fiber Characterization Tests

To determine the mechanical characteristics of the fibers used (metallic and polypropylene), direct tensile tests were conducted. The tests were performed on an "Ibertest" hydraulic press with controlled deformation at the Laboratory of Materials and Structures Modeling of Civil Engineering at the Mouloud Mammeri University of Tizi Ouzou in Algeria. The press is equipped with numerical control (as shown in the view provided in Figure 4). Geometric characteristics are input automatically, and the effective length of the fiber is 100 mm. The loading speed is set at 20 mm/min.

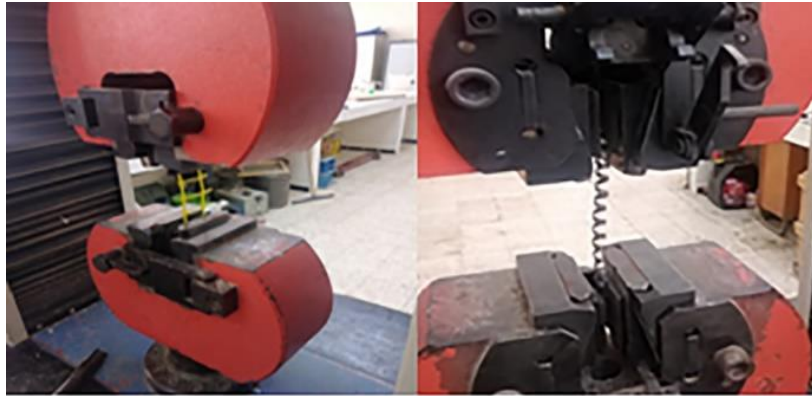


Figure 4. Test device view

Calculation of Mass Losses

For determining the mass loss as a function of the heating-cooling cycle, specimens are weighed before and after each heating-cooling cycle. The specimens from heating are weighed directly to avoid any rehydration phenomenon with the surrounding environment. The test aims to determine the material (or mass) loss experienced by the specimens during heating compared to their initial state (before heating). The mass loss expressed as a percentage is obtained using the following formula (1):

$$\text{mass loss} = \frac{M_0 - M_t}{M_0} \times 100\% \dots \dots \dots (1)$$

Thermal Tests

Each cycle (heating-cooling) consists of three phases (Figure 5). The first phase involves a temperature ramp-up at a rate of 1°C.min-1. The second phase is a constant temperature plateau within the furnace to homogenize the temperature within the specimens. It lasts for four hours. The final phase is a temperature decrease until reaching ambient value at an average speed of -1°C.min-1. This cooling phase of the specimens is not controlled. It occurs naturally depending on the temperature inside the furnace, which is kept closed. Indeed, the aim is to ensure that the damage induced in the concrete results solely from the effect of temperature.

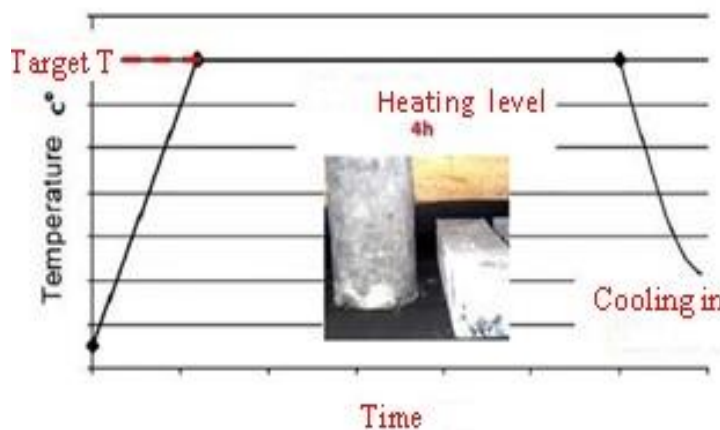


Figure 5. Heating – cooling cycles imposed on the specimens

The specimens are arranged within the furnace in such a way that heat is distributed evenly. This heat distribution is achieved through the furnace's ventilation system. The furnace control is carried out using a programmable controller connected to thermocouples. Figure 6 illustrates the arrangement of the specimens inside the furnace.



Figure 6. Arrangement of the test pieces inside the oven

Compression Tests

The compression tests are performed on an AUTOTEST hydraulic press with a maximum capacity of 2000 kN (Figure 7a), using cylindrical specimens with a diameter of 16 cm and a height of 32 cm (according to the NF EN12390-4 standard), as depicted in Figure 7b.



Figure 7a. Cylindrical test tubes



Figure 7b. With hydraulic press

Bending Tests (3-Point Bending)

Bending tests were conducted on prismatic specimens [10x10x40] cm³ using the 'Ibertest' machine to investigate the mechanical behavior of concrete reinforced with metallic fibers (MF) and polypropylene fibers (PPF) at elevated temperatures (600°C and 800°C), with a fiber volume fraction (W) of 0.8%, as well as plain concrete

(BT) without fibers ($W=0\%$). In total, 27 beams were tested. Figure 8 illustrates the static diagram of the three-point bending test.

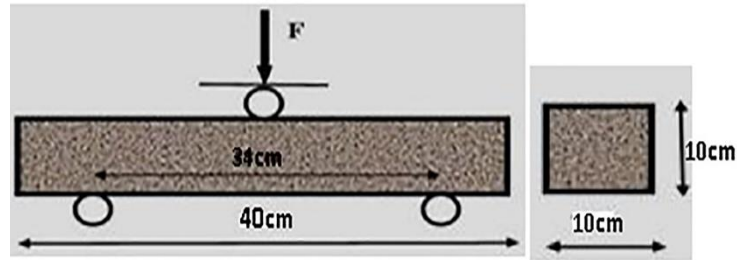


Figure 8. Static schema of the three-points bending test

Geometry and Composition of the Specimens

The specimens used for conducting three-point bending tests are prismatic specimens with dimensions $[10 \times 10 \times 40]$ cm³, with a width (l) of 10 cm, a height (h) of 10 cm, and a length (L) of 40 cm. The prismatic molds used are shown in Figure 9. The metallic fibers (MF) and polypropylene fibers (PPF) are randomly dispersed within the cementitious matrix. A vibrated mixture was used during casting.

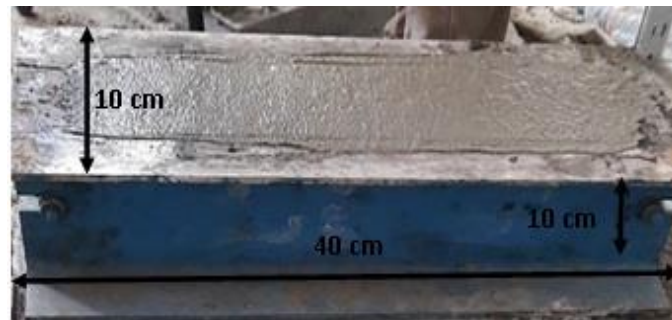


Figure 9. Prismatic molds used

Principle of the Test

After the heating-cooling cycle, the specimens of dimensions $[10 \times 10 \times 40]$ cm³ are subjected to flexural failure by applying a bending moment using an upper roller and two lower rollers. The specimens are carefully placed on the two lower support rollers and centered so that the longitudinal axis of the rollers (upper and lower) is orthogonal to the axis of the specimen (see Figure 10). In accordance with the NF EN ISO 527-2 standard [Afnor, 2001], loading is performed at a speed of 0.25 mm/min until failure. The maximum load as well as the force-deformation curve is recorded during the test.



Figure 10. The setup of the three-point bending test

Results and Discussions

Characterization Trials of Fibers under Tension

The tension stress-strain curves for three lengths of fibers (4 cm, 5 cm, and 6 cm) containing six undulations along the length are demonstrated in Figure 11. During the test, it is observed that the undulations of the fiber gradually open up until the fiber flattens. Beyond that, a ductile fracture of the steel is observed. The tensile strength increases as a function of the number of undulations: it reaches $R_m = 281$ MPa for a length $L = 6$ cm with 6 undulations shown in Figure 12.

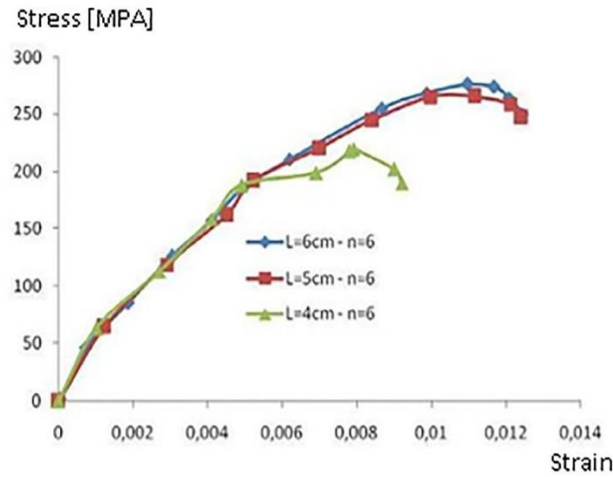


Figure 11. Average curve Stress-Strain



Figure 12. Fibers used $L = 6$ cm with 6 undulations

Figure 13 shows the mean value of three stress-strain curves as a function of deformation $\sigma = f(\epsilon)$. This study allowed us to determine the tensile strength of the polypropylene grid fibers used. It appears that the average resistance $R_m = 16.92$ MPa.

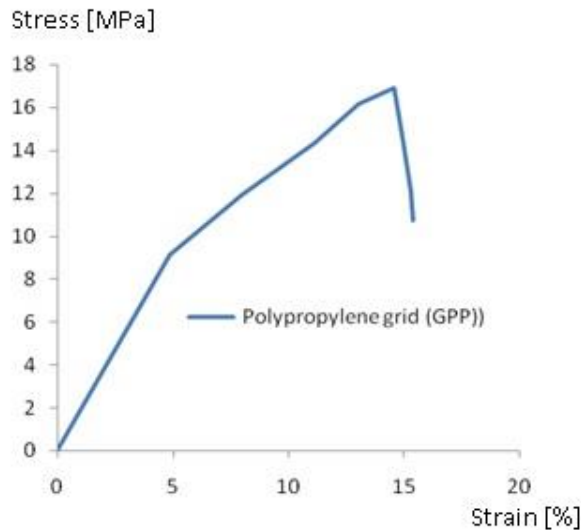


Figure 13. Average stress-strain curve of polypropylene fibers

Compression Tests

Mass Losses in Compression

Figure 14 illustrates the mass loss histogram under compression obtained by averaging three tests conducted on cylindrical specimens.

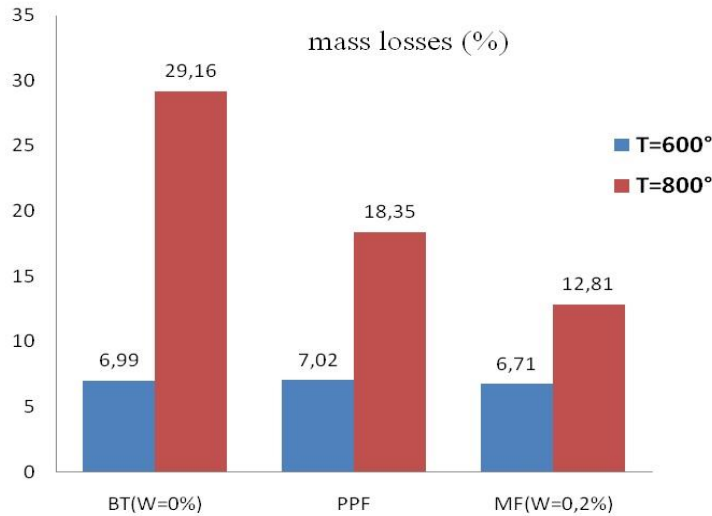


Figure 14. Mass losses of the different concretes studied

According to the histogram in Figure 14, it can be observed that as the temperature increases, the mass loss also increases. At 600°C, the various fiber-reinforced concretes (BT, CPPF and CMF) exhibited almost the same magnitude of mass loss, while at 800°C, the control concrete (BT with W=0%) and the polypropylene fiber-reinforced concrete (CPPF) showed a significant mass loss.

Compression Resistance

Figures 15, 16, and 17 illustrate the appearance of cylindrical specimens in plain concrete (BT), polypropylene fiber-reinforced concrete (CPPF), and metallic fiber-reinforced concrete (CMF) after being exposed to temperatures of 600°C and 800°C upon exiting the furnace.

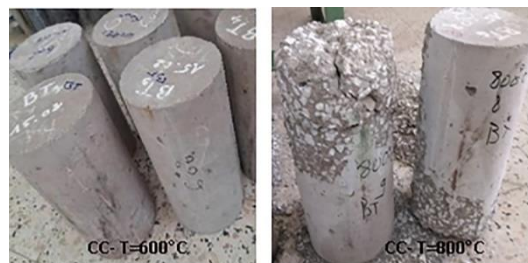


Figure 15. The appearance of the cylindrical specimens of the control concrete (BT) at the exit from the oven

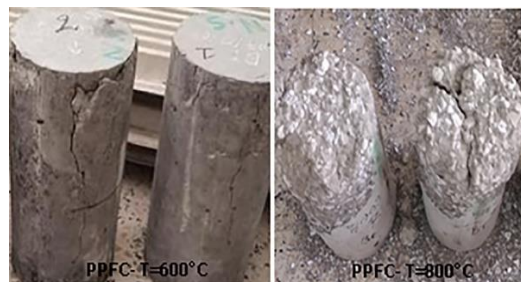


Figure 16. The appearance of polypropylene fiber concrete specimens (CPPF) at the exit of the oven

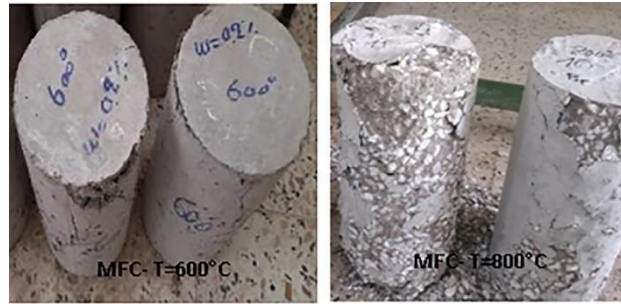


Figure 17. The appearance of fiber concrete specimen metallic (CMF) at the exit of the oven

Upon observing the appearance of the specimens upon exiting the furnace, we notice the occurrence of cracking in the form of crazing in the cases of metallic fiber-reinforced concrete (CMF), polypropylene fiber-reinforced concrete (CPPF), as well as in the case of plain concrete (CC). Furthermore, the polypropylene fiber-reinforced concrete (CFPP) subjected to a temperature of 800°C exhibited material detachment on half of the lateral surface of the cylinders. Figures 18, 19, and 20 respectively depict the overlay of average stress-strain curves under compression for plain concrete (BT), polypropylene fiber-reinforced concrete (CPPF), and metallic fiber-reinforced concrete (CMF) at temperatures of 20°C, 600°C, and 800°C.

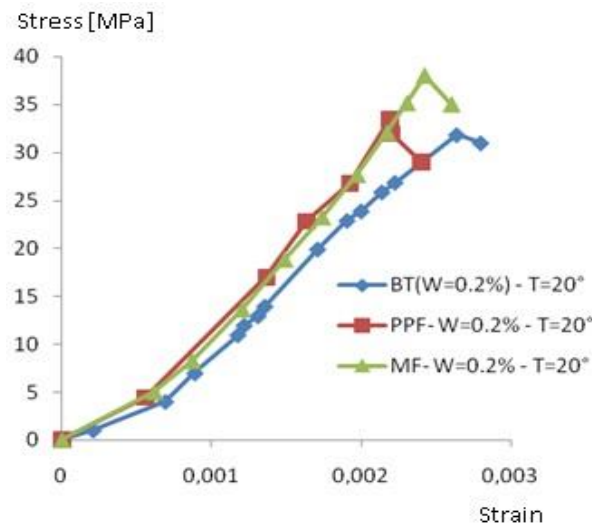


Figure 18. Stress-strain curves of concrete studied at T=20°C

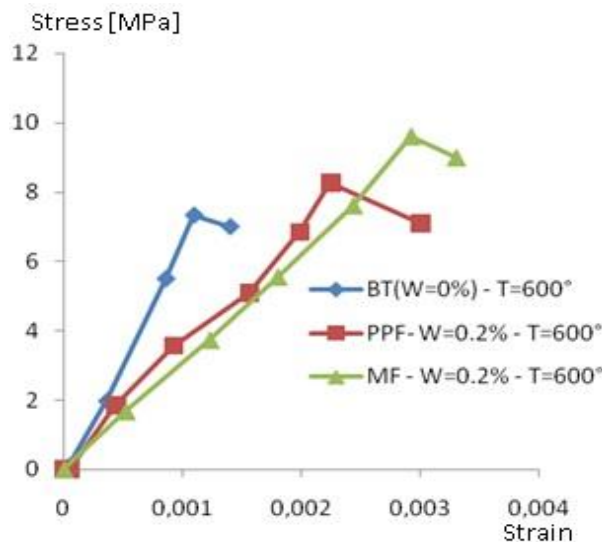


Figure 19. Stress-strain curves of concrete studied at T=600°C

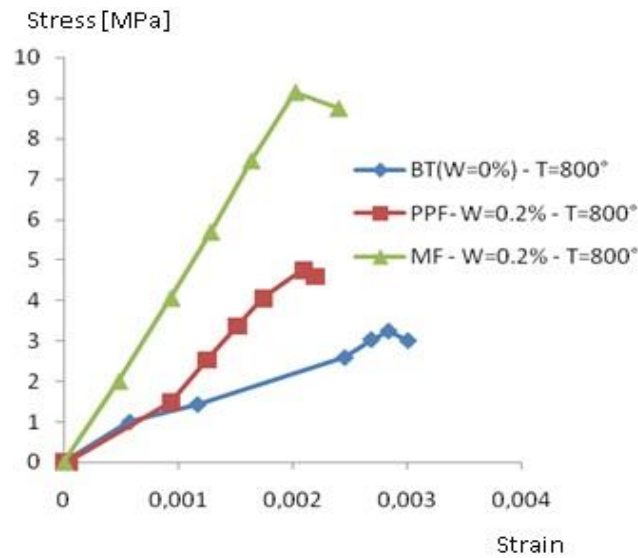


Figure 20. Stress-strain curves of concrete studied at T=800°C

According to the curves in Figures 18, 19, and 20 presenting stress-strain behavior under compression, for all types of concrete studied (BT, CPPF and CMF) subjected to temperatures of 20°C, 600°C, and 800°C, it was observed that concretes subjected to heating-cooling cycles at temperatures of 600°C and 800°C exhibited lower strengths as well as a decrease in the slope of the stress-strain curves compared to concretes that were not subjected to such heating-cooling cycles. As for steel fiber-reinforced concrete (CMF) and polypropylene fiber-reinforced concrete (CPPF), an improvement in deformability was observed. Figure 21 illustrates the histogram of compressive strength of the different concrete types studied (BT, CMF and CPPF) subjected to temperatures of 20°C, 600°C, and 800°C.

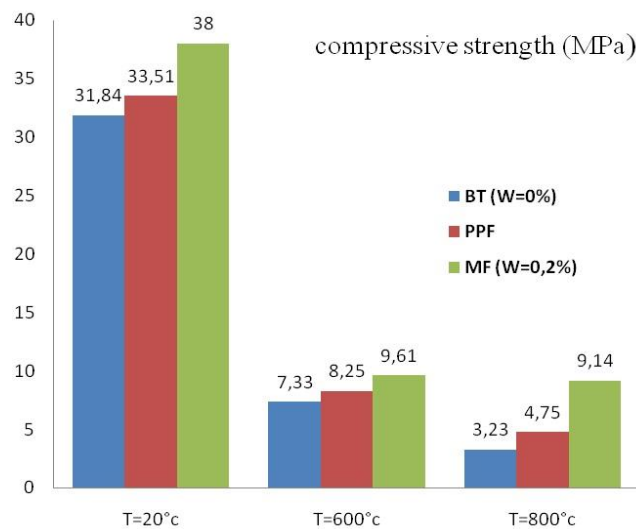


Figure 21. Compressive strength of the different concretes studied

According to Figure 20, for all temperatures, it is observed that steel fiber-reinforced concrete (CMF) exhibits higher compressive strength compared to polypropylene fiber-reinforced concrete (CPPF) and the control concrete BT (without fibers). At 800°C, there is a significant drop in the strength of the concretes (CMF and CPPF) compared to those at 20°C. This drop is approximately 76% for steel fiber-reinforced concrete (CMF) and 86% for polypropylene fiber-reinforced concrete (CPPF).

Bending Tests (3-Point Bending)

Figures 22, 23, and 24 illustrate examples of the failure mode of the beams tested in control concrete BT (W=0%), polypropylene fiber-reinforced concrete (CPPF), and steel fiber-reinforced concrete (CMF) after being exposed to temperatures of 20°C, 600°C, and 800°C.



Figure 23. Exemple des poutres testées à 600°C

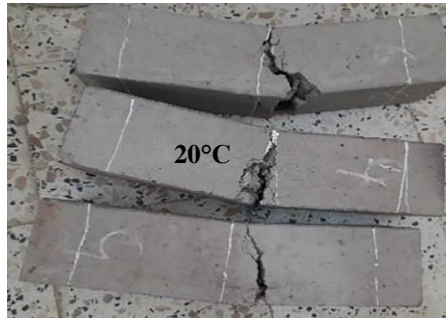


Figure 22. Exemple des poutres testées à 20°C

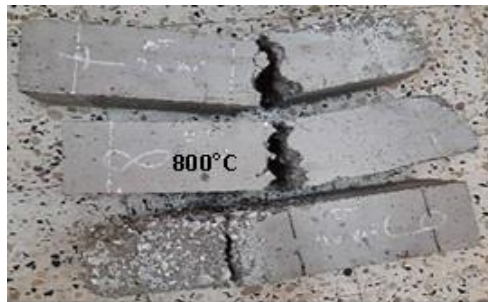


Figure 24. Exemple des poutres testées à 800°C

Loss of Mass in Flexure

Figure 25 illustrates the histogram of loss of mass in flexure obtained by averaging three tests conducted on the prismatic beams.

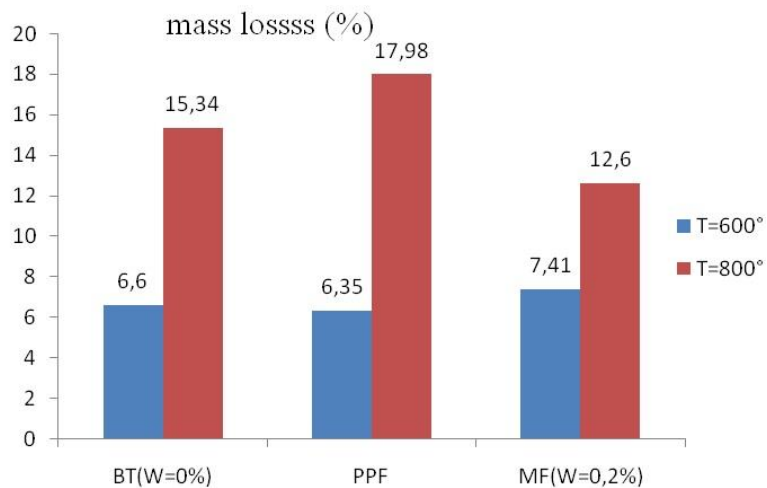


Figure 25. Mass losses of the different concretes studied

According to the histogram in Figure 25, it is observed that the loss of mass increases proportionally with the rise in temperature. At 600°C, the various fiber-reinforced concretes (BT (W=0%), CPPF and CMF) recorded similar mass losses, while at 800°C, the control concrete BT (without fibers) and polypropylene fiber-reinforced concrete (CPPF) experienced significant mass losses.

Bending Resistance

The Figures 26, 27, and 28 respectively present the superimposition of the average force-deformation curves in flexure for the control concrete BT (W=0%), polypropylene fiber-reinforced concrete (CPPF), and steel fiber-reinforced concrete (CMF) at temperatures of 20°C, 600°C, and 800°C.

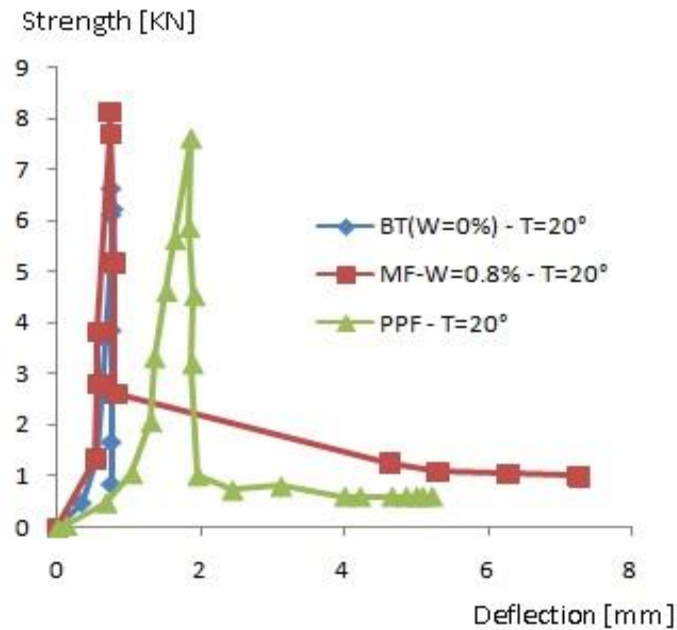


Figure 26. Superposition of the average strength-deflection curves of the beams tested at 20°C

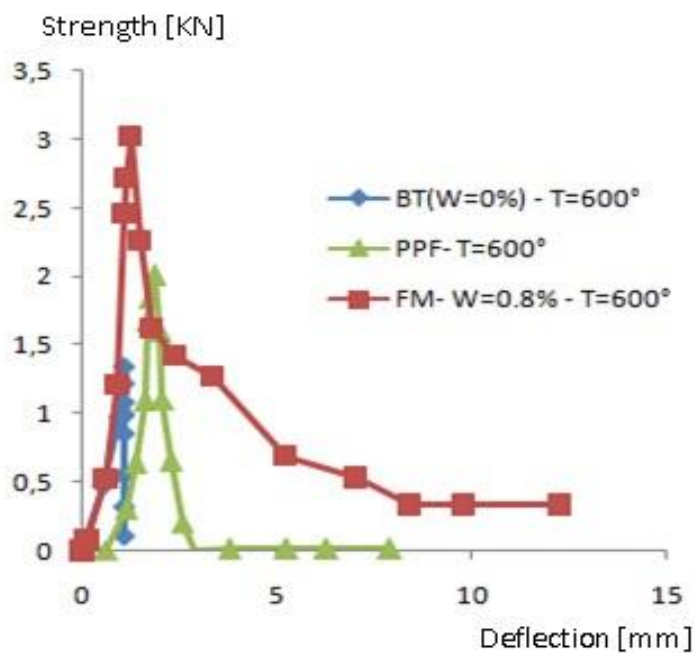


Figure 27. Superposition of the average strength-deflection curves of the beams tested at 600°C

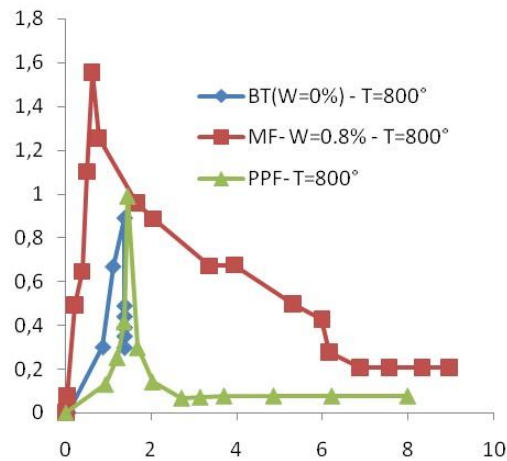


Figure 28. Superposition of the average strength-deflection curves of the beams tested at 800°C

Figures 26, 27, and 28 illustrate the relationship between force and deformation (deflection) during the flexural behavior of fiber-reinforced concretes. They reveal that the behavior of fiber-reinforced concretes can be divided into two distinct phases: an initial linear phase corresponding to elasticity, followed by a post-cracking phase where the fibers continue to provide resistance. These graphs demonstrate that steel fiber-reinforced concrete (CMF) exhibits better flexural performance at all studied temperatures. Particularly, its behavior after the peak strength is superior to that of plain concrete (BT, W=0%) and polypropylene fiber-reinforced concrete (CPPF). Additionally, a significant drop in strength is observed for all types of concretes (BT, CPPF and CMF) at a temperature of 800°C. Figure 29 illustrates the histogram of compressive strength of the different concrete types studied (BT, CMF, CPPF) subjected to temperatures of 20°C, 600°C, and 800°C.

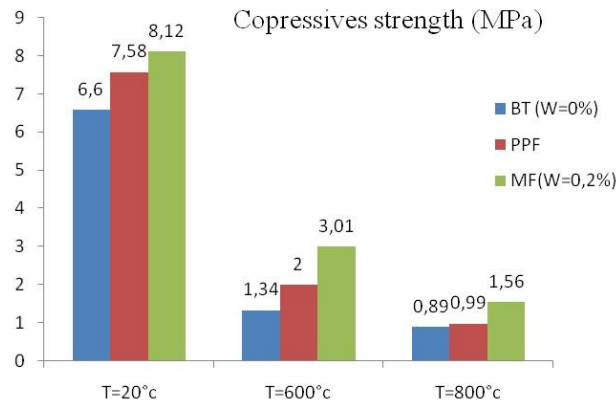


Figure 29. Compressive strength of the different concretes studied

According to the data from Figure 29, it is notable that metallic fiber reinforced concrete (CMF) exhibits higher flexural strength compared to polypropylene fiber reinforced concrete (CPPF) and unreinforced concrete (BT). At a temperature of 800°C, a significant decrease in strength is observed for the concretes (CMF and CPPF) compared to that at 20°C. This decrease represents approximately 81% for metallic fiber reinforced concrete (CMF) and 87% for polypropylene fiber reinforced concrete (CPPF).

Conclusion

The objective of this experimental study is to contribute to a better understanding of the behavior of recycled fiber-reinforced concrete exposed to high temperatures of 600°C and 800°C, as well as the influence of steel fibers (MF) and polypropylene fibers (PPF) on this behavior in compression and flexure. Concrete samples, whether containing fibers or not, were manufactured for testing purposes. The results of this experimental study have allowed us to draw the following conclusions:

The results obtained are very encouraging. Indeed, they indicate an increase in the tensile strength of steel fibers (MF) correlated with the fiber length and the number of spirals. The best performance is observed with fibers

measuring 6 cm in length and having 6 spirals. The loss of mass in compression and flexure calculated for steel fiber-reinforced concrete (CMF), polypropylene fiber-reinforced concrete (CPPF), and plain concrete (BT, W=0%) allowed us to observe that as the temperature increases, the loss of mass also increases. At 600°C, the different fiber-reinforced concretes (BT, CMF and CPPF) exhibited almost the same magnitude of mass loss; this significant mass loss corresponds to the departure of chemically bound water. Whereas at 800°C, it was the polypropylene fiber-reinforced concrete (CPPF) that experienced significant mass loss, along with the control concrete BT (without fibers), caused by the degradation of the cementitious matrix. During the examination of compression tests on cylindrical specimens after removal from the furnace, cracking in the form of crazing was observed in the case of steel fiber-reinforced concrete CMF), polypropylene fiber-reinforced concrete (CPPF), as well as in the case of plain concrete BT (W=0%). Additionally, the plain concrete subjected to a temperature of 800°C exhibited material spalling on half of the lateral surface of the specimens. For all temperatures, it is noted that steel fiber-reinforced concrete (CMF) exhibited higher compressive and flexural strengths compared to polypropylene fiber-reinforced concrete (CPPF) as well as the plain concrete BT (without fibers). At 800°C, there is a significant drop in both compressive and flexural strength for all types of concrete, compared to the strengths at 20°C.

Finally, based on the results obtained, it can be concluded that the use of steel fibers (machining chips from steel parts) increases the fire resistance of concrete. Indeed, the chip fibers limit the opening of cracks, thus providing effective protection to traditional reinforcements against thermal radiation. From a broader perspective, it would be interesting to conduct tests on real large-scale specimens, to use flat chip fibers instead of corrugated fibers to reduce voids (cavities) in the cement paste, and also to combine these fibers with traditional reinforcement.

Scientific Ethics Declaration

The authors declare that the scientific ethical and legal responsibility of this article published in EPSTEM. Journal belongs to the authors.

Acknowledgements or Notes

* This article was presented as a poster presentation at the International Conference on Technology, Engineering and Science (www.icontes.net) held in Antalya/Turkey on November 14-17, 2024.

* The team from our Laboratory of Materials and Structures Modeling in Civil Engineering (L2MSGC) thanks you for giving us the opportunity to participate in the ICONTES 2024 conference and to contribute to our research together. We also express our gratitude to the reviewers for examining this work with the aim of improving it.

References

- Atlaoui, D., & Bouafia, Y. (2017). Experimental characterization of concrete beams elements reinforced by long fiber chips. *Journal of Adhesion Science and Technology*, 31(8), 844-857.
- Atlaoui, D., & Ghouilem, K. (2023). Effect of chipped fiber languor on the bending behavior of concrete beam elements. *Journal of Applied Engineering Sciences*, 13(2), 155-162.
- Atlaoui, D., Adjrad, A., & Bouafia, Y. (2023). Effect of recovered fibers on the behavior of concrete in tension. *Slovak Journal of Civil Engineering*, 31(4), 26-33.
- Bouafia, Y., Kachi, M. S., Atlaoui, D., & Djebali, S. (2012). Study of mechanical behavior of concrete in direct tensile fiber chips. *Applied Mechanics and Materials*, 146, 64-73.
- Castillo, C., & Durrani, A. J. (1990). *Effect of transient high temperature on high-strength concrete* (pp.47-53). Rice University.
- Coke, F., & Venstermans, J. (1977). Béton renforcé de fibres d'acier. *CSTC Magazine (Bruxelles)*, (3), 2-19.
- Dias, W. P. S., Khoury, G. A., & Sullivan, P. J. E. (1990). Mechanical properties of hardened cement paste exposed to temperature up to 700°C. *ACI Materials Journal*, 87(2), 160-166.
- Diederichs, U., & Jumppanen, U. M. (1992). High temperature properties and spalling behavior of high-strength concrete. In *Verlog für architektur und techn. wissenheften* (pp.191-197). Ernst & schn.
- Djebali, S., Atlaoui, D., & Bouafia, Y. (2011). Caractérisation en traction directe du béton de fibres métalliques. *Matériaux & Techniques*, 99(3), 327-338.

- Djebali, S., Bouafia, Y., Atlaoui, D., & Bilek, A. (2011). Study of mechanical behavior of chips reinforced concrete. *Advanced Materials Research*, 324, 360-363.
- Djebali, S., Bouafia, Y., Atlaoui, D., & Bilek, A. (2011). Study of mechanical behavior of chips reinforced concrete. *Advanced Materials Research*, 324, 360-363.
- Dreux, G., & Festa, J. (2007). *Nouveauguide du bétonet des constituants*. Huitième (Ed.).
- Hager, I. (2004). *Comportementà haute température des beton sà haute performance-évolution des principales propriétés mécaniques*. Doctoral dissertation.
- Noumowe, A. (2005). Mechanical properties and microstructure of high strength concrete containing polypropylene fibres exposed to temperatures up to 200 C. *Cement and Concrete Research*, 35(11), 2192-2198.
- Phan, L. T. (2002). High-strength concrete at high temperature-an overview, national institute of standards and technology. *High Performance Concrete 6th International Symposium Proceeding*, 1.
- Pimienta, P. (2000). Le comportement au feu des BHP, synthèse des travaux du projet national sur les bétons à hautes performances In *Presses de l'école nationale des ponts et chaussées* (pp.77-124). BHB.
- Pliya, B. (2010). *Contribution des fibres de polypropylène et métalliques à l'amélioration du comportement du béton soumis à une température élevée*. Doctoral dissertation, Cergy-Pontoise.
- Sana, T., & Abdul, H. (2013). Effect of elevated temperatures on compressive and tensile strengths of reactive powder concrete. *Journal of Engineering and Development*, 17(4), 259-278.
- Serbescu, A., Guadagnini, M., & Pilakoutas, K. (2013). Mechanical characterization of basalt FRPR ebars and long-term strength predictive model. *Journal of Composites for Construction*, 19(2), 04014037.
- Serrano, R., Cobo, A., Prieto, M. I., & de las Nieves González, M. (2016). Analysis of fire resistance of concrete with polypropylene or steel fibers. *Construction and Building Materials*, 122, 302-309.
- Shallal, M. A., & Al-Owaisy, S. R. (2007). Strength and elasticity of steel fiber reinforced concrete at high temperatures. *Journal of Engineering and Sustainable Development*, 11(2), 125-133.
- Sorensen, C., Berge, E., & Nikolaisen, E. B. (2014). Investigation of fiber distribution in concrete batches discharged from ready-mix truck. *International Journal of Concrete Structures and Materials*, 8(4), 279-287.
- Tadepalli, P.R., Mo, Y., & Hsu, T.T. (2013). Mechanical properties of steel fiber concrete. *Magazine of Concrete Research*, 65(8), 462-474.
- Tai, Y. S., Pan, H. H., & Kung, Y. N. (2011). Mechanical properties of steel fiber reinforced reactive powder concrete following exposure to high temperature reaching 800 C. *Nuclear Engineering and Design*, 241(7), 2416-2424.
- Tshimanga, M. K. (2007). *Influence des paramètres de formulation sur le comportement à haute température des bétons*. Doctoral dissertation, Cergy-Pontoise.
- Wang, H. T., & Wang, L. C. (2013). Experimental study on static and dynamic mechanical properties of steel fiber reinforced lightweight aggregate concrete. *Construction and Building Materials*, 38, 1146-1151.
- Yermak, N., Pliya, P., Beaucour, A. L., Simon, A., & Noumowé, A. (2017). Influence of steel and/or polypropylene fibres on the behaviour of concrete at high temperature: Spalling, transfer and mechanical properties. *Construction and Building Materials*, 132, 240-250.

Author Information

Atlaoui Djamel

Department of Civil Engineering, Laboratory of Modeling of and Structures in Civil Engineering (L2MSGC), University 'Mouloud Mammeri' of Tizi Ouzou, 15000, Algeria.

Contact e-mail: djamal.atlaoui@umt.dz

Bouafia Youcef

Department of Civil Engineering, Laboratory of Modeling of Materials and Structures in Civil Engineering (L2MSGC), University 'Mouloud Mammeri' of Tizi Ouzou, 15000, Algeria.

Ghoulem Kamel

Department of Civil Engineering, Faculty of Construction Engineering Laboratory of Geomaterial, Environment and Amenagement (LGEA), University of Mouloud Mammeri, Tizi Ouzou, Algeria.

To cite this article:

Djamel, A., Youcef, B. & Kamel, G. (2024). The effect of high temperatures on the compression and flexural characteristics of recycled fiber-reinforced concrete. *The Eurasia Proceedings of Science, Technology, Engineering & Mathematics (EPSTEM)*, 32, 575-590.